We are IntechOpen,
the world's leading publisher of Open Access books
Built by scientists, for scientists

6,900
Open access books available

185,000
International authors and editors

200M
Downloads

Our authors are among the

154
Countries delivered to

TOP 1%
most cited scientists

12.2%
Contributors from top 500 universities

CLARIVATE ANALYTICS
BOOK CITATION INDEX
INDEXED

WEB OF SCIENCE™

Selection of our books indexed in the Book Citation Index
in Web of Science™ Core Collection (BKCI)

Interested in publishing with us?
Contact book.department@intechopen.com

Numbers displayed above are based on latest data collected.
For more information visit www.intechopen.com

Simulated Nanoscale Peeling Process of Monolayer Graphene Sheet - Effect of Edge Structure and Lifting Position

Naruo Sasaki[1], Hideaki Okamoto, Shingen Masuda,
Kouji Miura* and Noriaki Itamura
Seikei University,
*Aichi University of Education,
Japan

1. Introduction

Adhesion and peeling phenomena play important roles for connecting two objects regardless of whether they are inorganic, organic or biological materials, which contributes to buliding up microscopic devices. The carbon nanostructures such as carbon nanotube (CNT) and graphene have recently attracted great interests as the components of the electronic, magnetic and optical devices. We have so far studied the peeling mechanics of the carbon nanotube (CNT) adsorbed onto the graphite surface both theoretically (Sasaki et al., 2006, 2008, 2009b) and experimentally (Ishikawa et al., 2008, 2009). It is clarified that the transition from the line- to the point-contact between the CNT and the graphite surface occurs during the peeling process. The CNT on the sub-microscale has the same size as the spatulae of the microscopic hairs aligned on the gecko foot (Autumn et al., 2000, 2002). Therefore the study of the peeling process of the nano-scale objects such as CNT is useful for not only developing the gecko-foot-mimic adhesives (Qu et al., 2008) but also understanding the elementary process of adhesion.

On the other hand, since the success of its experimental isolation (Novoselov et al., 2004), the potential of various application of the graphene such as the components of the electronic devices (Novoselov et al., 2005, Geim et al., 2007), has been discussed by many researchers. There is also a possibility that its adhesion with the substrate is applied to the adhesive tape at nanoscale. Therefore the peeling mechanics of the graphene sheet is very important, which can be regarded as the elementary process of the macroscopic sticky tape such as the gecko-foot-mimic adhesives (Autumn et al., 2000, 2002, Qu et al., 2008), or that of the microscopic extension of the crack in the fracture process. In our preliminary experiments, we have already succeeded in peeling the multilayered graphene plate with a thickness of several μm by using atomic-force microscopy tip. Here the two-component epoxy resin adhesive is used to bond the graphene plate to the AFM tip. Here the standard Si_3N_4 tip for the contact AFM experiment is used. The junction formed between the AFM tip and the graphene should be mechanically rigid enough to measure the elasticity of the graphene

---

[1]Corresponding author: naru@st.seikei.ac.jp

sheet during the peeling process. The two-component epoxy resin adhesive satisfies the above condition. If the thickness of the peeled graphene plate is reduced, the comparison between the present simulation and the experiment will become possible.

Therefore, in this chapter, ahead of experiment, we have theoretically reported the nanoscale peeling behaviors of the monolayer graphene sheet based on the molecular mechanics simulation (Sasaki et al., 2009a, 2010). The peeling force curve exhibits the nanoscale change of the graphene shape from the surface to the line contact. The center position and the left edge are chosen as the lifting position. In Section 3, the peeling of the monolayer graphene sheet with the armchair edge for lifting the center position is discussed. In Secs. 4 and 5, the peeling of the monolayer graphene sheet with the armchair- and zigzag-edge for lifting the edge position is discussed, respectively.

2. Model and method of simulation

In the simulation, a rectangular-shaped monolayer graphene sheet with each side of 38 Å $\times$ 20 – 21 Å, comprised of 310 carbon atoms, is peeled from the rigid rectangular graphene sheet (which is called, the 'graphite surface,' hereafter) with each side of 164-165 Å $\times$ 58 Å, comprised of 3536 carbon atoms [Fig. 1(a)]. First, both the above graphene sheets are separately optimized by minimizing the covalent bonding energy described by the Tersoff potential energy (Tersoff, 1988), V_{cov}, using the Polak-Rebiere-type conjugate gradient (CG) method (Press et al., 1999). Here the convergence criterion is set so that the maximum of absolute value of all the forces acting on the movable atoms, becomes lower than 10^{-5} eV/Å. Next, the graphene sheet is put and adsorbed onto the graphite surface, so that the AB stacking registry between the graphene sheet and the graphite surface is satisfied as shown in Figs. 1(b) and 1(c). Here the green-colored six-membered ring at the center position or the outermost left edge of the graphene sheet is assumed to be attached to the AFM tip apex [Fig. 1(a)], and then it is gradually moved upward along the z direction, parallel to the [0001] axis, by 0.1 Å. For each lifting position of the graphene sheet, z, the total energy V_{total} $=V_{cov} + V_{vdW}$, is minimized using the CG method, where V_{vdW} is the nonbonding vdW interaction described by the modified Lennard-Jones (LJ) potential energy (Lu et al., 1988, Stoddard and Ford, 1973), acting between the graphene sheet and the graphite surface. Thus the optimized positions of the movable carbon atoms of the graphene sheet, (x, y, z), the vertical peeling force F_z, and the lateral sliding forces F_x and F_y, acting on the lifting center, are calculated during the peeling process. In this paper, the graphene sheets with armchair- [Fig. 1(b)] and zigzag-edges [Fig. 1(c)] are discussed.

3. Center-lifting case of armchair-edge graphene

When the six-membered ring located at the center position of the monolayer graphene sheet is lifted, the graphene sheet exhibits the characteristic transition of its shape during the peeling process within the x-z plane as illustrated in Figs. 2A-2J, corresponding to Figs. 3A-3J, the vertical force acting on the lifting center position F_z plotted as a function of the displacement from the initial position along z-direction, z. At first the monolayer graphene sheet takes an initial planar structure parallel to the rigid graphite surface [Fig. 2A: $z = 0$ Å]. Here the surface contact is formed between the graphene sheet and the graphite surface. The vertical force F_z is zero [Fig. 3A]. Just after the beginning of the peeling [Fig. 2B: $z = 2.0$ Å], the attractive interaction force takes the minimum value, –3.1eV/Å [Fig. 3B].
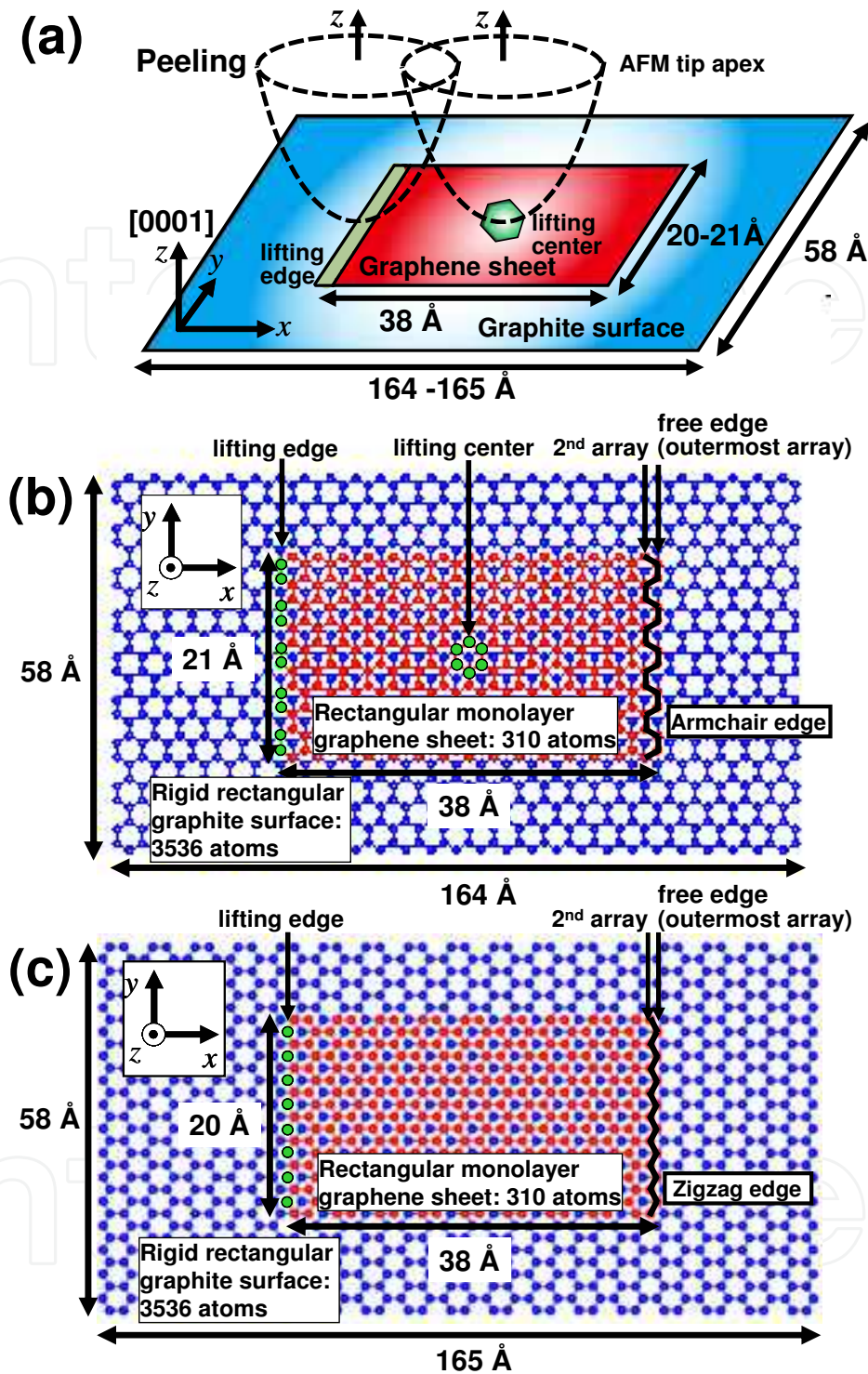
Fig. 1. (a) The schematic illustration of the model of the monolayer graphene sheet physically adsorbed onto the rigid graphite surface used in the simulation. The green-colored six-membered ring at the center position or left edge of the graphene sheet is assumed to be adsorbed onto the atomic force miroscopy tip apex indicated by broken lines, and it is moved upward along the z (or [0001]) direction, by $z = 0.1$ Å. Initial AB stacking registry of the red-colored graphene sheet with (b) armchair and (c) zigzag edge adsorbed onto the blue-colored graphite surface within the x - y plane.
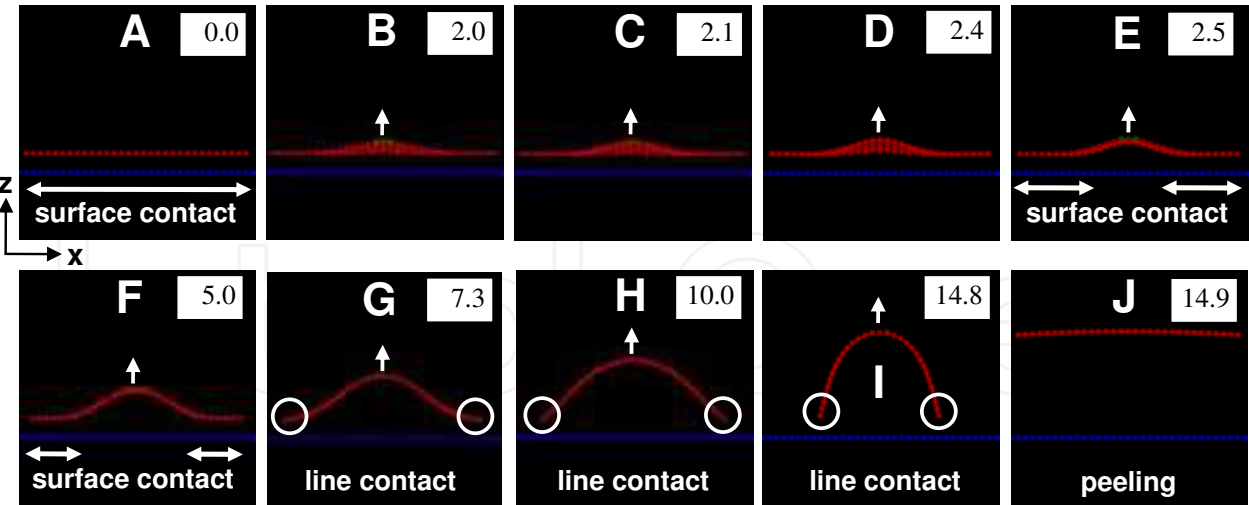
Fig. 2. The transition of the shape of the monolayer graphene sheet during the peeling process from A to J within the *x* - *z* plane. The red-colored graphene sheet and blue-colored graphite surface are shown. The displacement of the lifting center position from the initial position, *z* [Å], is indicated on the upper-right positions of each picture.
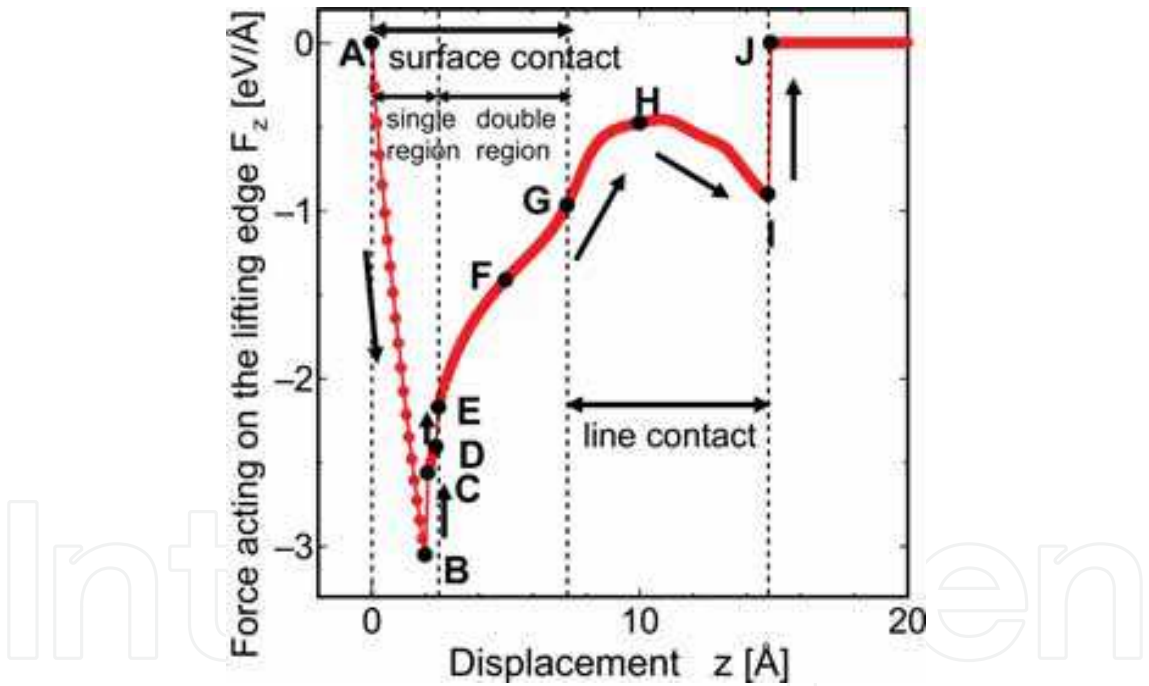

Fig. 3. The vertical force, F_z, acting on the center six-membered ring, plotted as a function of the lifting displacement *z*. The positions A-J correspond to those of Fig.2.

Between z = 2.0 Å and 2.1 Å, the first discrete partial peeling of the graphene occurs [Figs. 2B → 2C], which produces the 1st discontinuous jump in the force curve [Figs. 3B → 3C]. The partial peeled area around the lifting center of the graphene is shown in Figs. 4B → 4C. Then, between z = 2.4 Å and 2.5 Å, the second discrete partial peeling of the graphene occurs [Figs. 2D → 2E], which produces the 2nd discontinuous jump in the force curve [Figs. 3D → 3E]. The partial peeled area of the graphene is shown in Figs. 4D → 4E. Which of these two areas is peeled first is expected to be actually the stochastic process under the

room temperature condition. Now the surface contact region is split into the left and right sections [Fig. 2E]. After the two discrete jumps, F_z increases as the peeling proceeds, since the attractive surface contact region gradually decreases [Fig. 2F: z = 5.0 Å]. Then the surface contact continuously turns into the line contact at z = 7.3 Å [Fig. 2G]. Here the 'line contact' is defined by the following two criteria: 1) The carbon atoms on the left and right outermost arrays of the graphene sheet [Fig. 1(b)] receive the repulsive interaction force from the graphite surface. 2) The carbon atoms on the second arrays [Fig. 1(b)] next to the outermost arrays receive the attractive interaction force. As illustrated in Fig. 5, the average forces acting on one carbon atom on the outermost and the second arrays satisfy the above criteria at z = 7.3 Å, which corresponds to Fig. 2G.
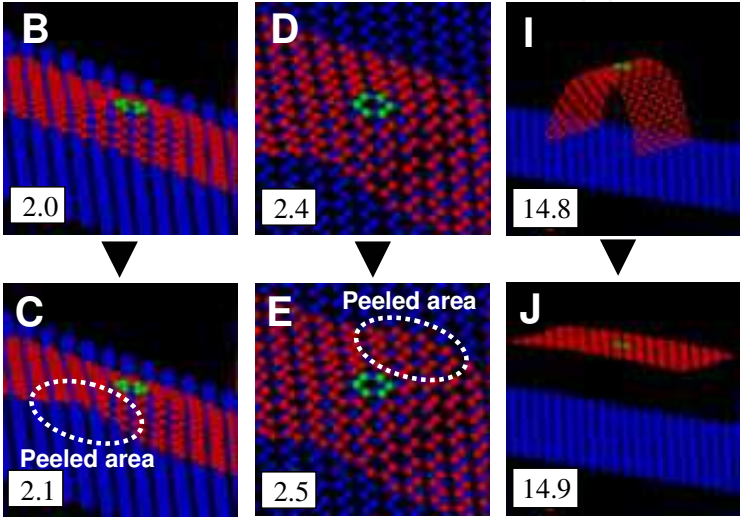

Fig. 4. The atomic structures of the graphene sheet just before and after the discrete change, B $\rightarrow$ C, D $\rightarrow$ E, and I $\rightarrow$ J. The regions surrounded by dotted ellipses show the partial peeled areas.
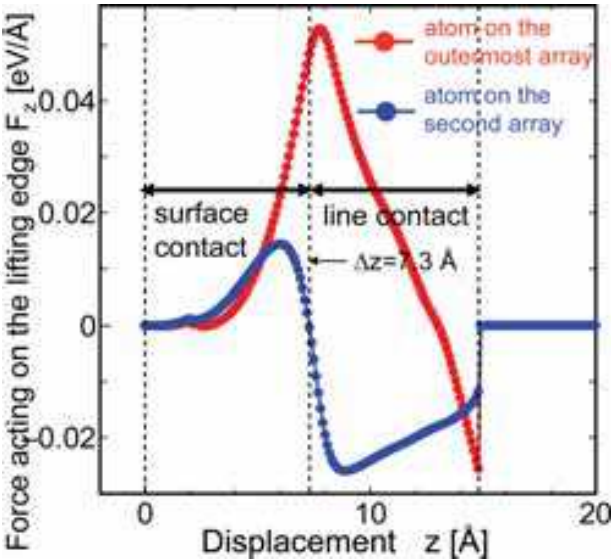

Fig. 5. The averaged forces acting on one atom on the left and right outermost arrays (red-colored) and those on the left and right second arrays (blue-colored), as a function of the displacement of the lifting center position from the initial position, z [Å].

Once the line contacts are formed between the free edges (outermost arrays) of the peeled graphene sheet and the graphite surface, they clearly slide on the graphite surface as indicated by a circle in Figs. 2G → 2H → 2I with a rapid increase of the bending of the graphene sheet. Within x-y plane, the right outermost array of the graphene sheet slides nearly straightforward along -x direction, not so sensitive to the lattice structure of the surface as illustrated in Figs. 6(a) and 6(b), which show the trajectories of the two carbon atoms on the right outermost array illustrated in Fig. 1(b). The sliding of the outermost arrays during G and I appears much more clearly than that during A and G, During H and I, the decrease of F_z [Figs. 3H and 3I] can be explained by the decrease of the repulsive force acting on the carbon atoms on the left and right edges of the graphene sheet as shown in Fig. 5, that's to say, the relative increase of the effect of the attractive interaction force.
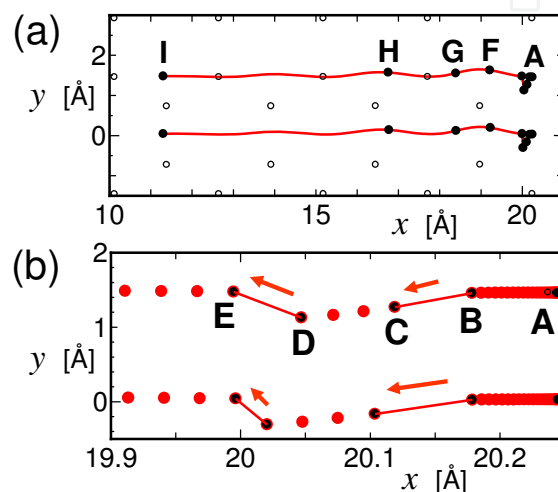

Fig. 6. The trajectory of the two carbon atoms on the right free edge (outermost array) indicated by white circles in Fig. 1(b). (a) The whole trajectory A → I, and (b) the part of the trajectory A → E, including the discrete jumps, B → C and D → E, are indicated. White circles mean carbon atoms of the graphite surface. The indices A – I correspond to those in Fig. 2.
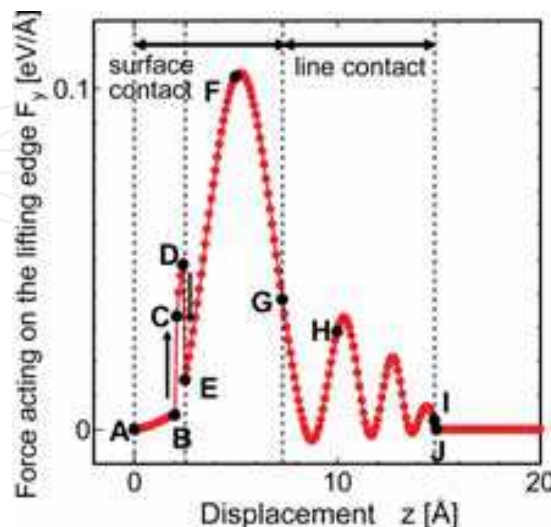

Fig. 7. The lateral force, F_y, acting on the center six-membered ring, plotted as a function of the displacement z. The positions A-J correspond to those of Fig. 2.

When the bending of the graphene sheet becomes larger than a certain range, both the left and right line contacts break and the graphene sheet is completely peeled from the surface [Figs. 2I → 2J: $z = 14.8$ Å → 14.9 Å], which produces the 3rd discontinuous jump in the force curve [Figs. 3I → 3J]. As illustrated in Figs. 2I → 2J, and Figs. 4I → 4J, the graphene sheet exhibits the transition from the arched shape to the planer shape.

Thus the vertical peeling force F_z exhibits the characteristic shape as shown in Fig. 3, which reflects the transition from the surface to the line contact between the graphene sheet and the graphite surface. On the other hand, the lateral sliding force F_x is zero due to the structural symmetry of the system. However, the lateral sliding force F_y shows a finite value with an oscillation whose period and amplitude decreases as z increases. This oscillation of Fig. 7 reflects the trajectory of the graphene edges illustrated in Fig. 6 at the graphene - substrate interface during the peeling process. The maximum lateral force $F_y \approx 0.1$ eV/Å which is only about 3 % of the absolute value of the maximum adhesion force $|F_z| = 3.1$ eV/Å.

4. Edge-lifting case of armchair-edge graphene

4.1 Nano-scale peeling along vertical direction

When the left edge of the monolayer graphene sheet with armchair edge [Fig. 1(b)] is lifted, the shape of the graphene sheet markedly changes during the peeling process within the x-z plane as illustrated in Figs. 8A-8J, corresponding to Figs. 9(a)A-9(a)J, the vertical force acting on the lifting edge F_z plotted as a function of the edge height z.
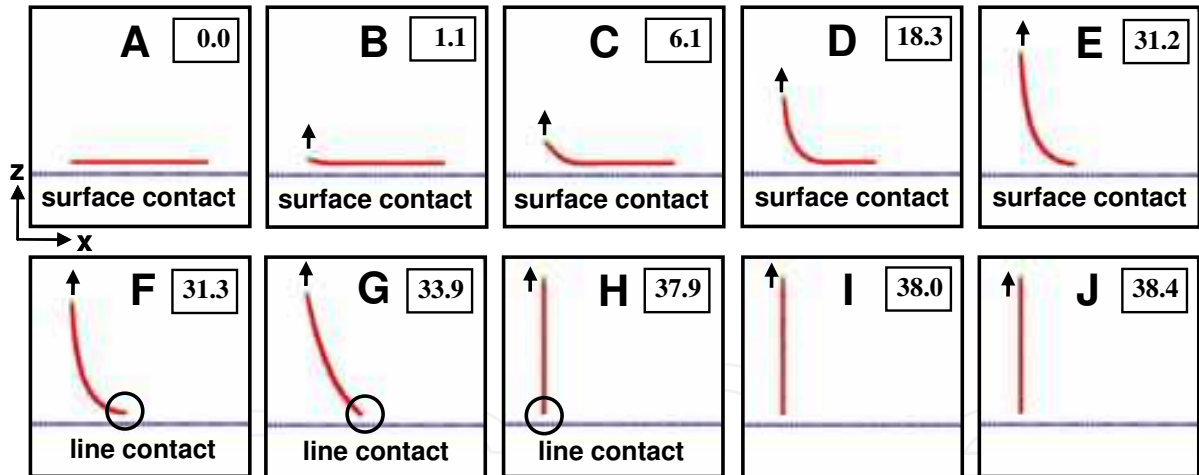

Fig. 8. The transition of the shape of the monolayer graphene sheet with free edge of armchair-type during the peeling process from A to J within the x - z plane. The red-colored graphene sheet and blue-colored graphite surface are shown. The height of the lifting left edge z [Å] are indicated on the upper-right positions of each picture.

Surface-contact region At first the monolayer graphene sheet takes an initial planar structure parallel to the rigid graphite surface [Fig. 8A: $z = 0$ Å], and the vertical force F_z is zero [Fig. 9(a)A], which means the graphene sheet completely takes the surface contact with the graphite surface. Just after the start of the peeling [Fig. 8B: $z = 1.1$ Å], the attractive interaction force $|F_z|$ becomes the maximum, 0.74 eV/Å [Fig. 9(a)B]. After that the surface contact area gradually decreases as the peeling proceeds [Figs. 8C-8E], where Fig. 9(a) exhibits the atomic-scale zigzag structures [Figs. 9(a)C-E], which will be explained in Section 4.2.
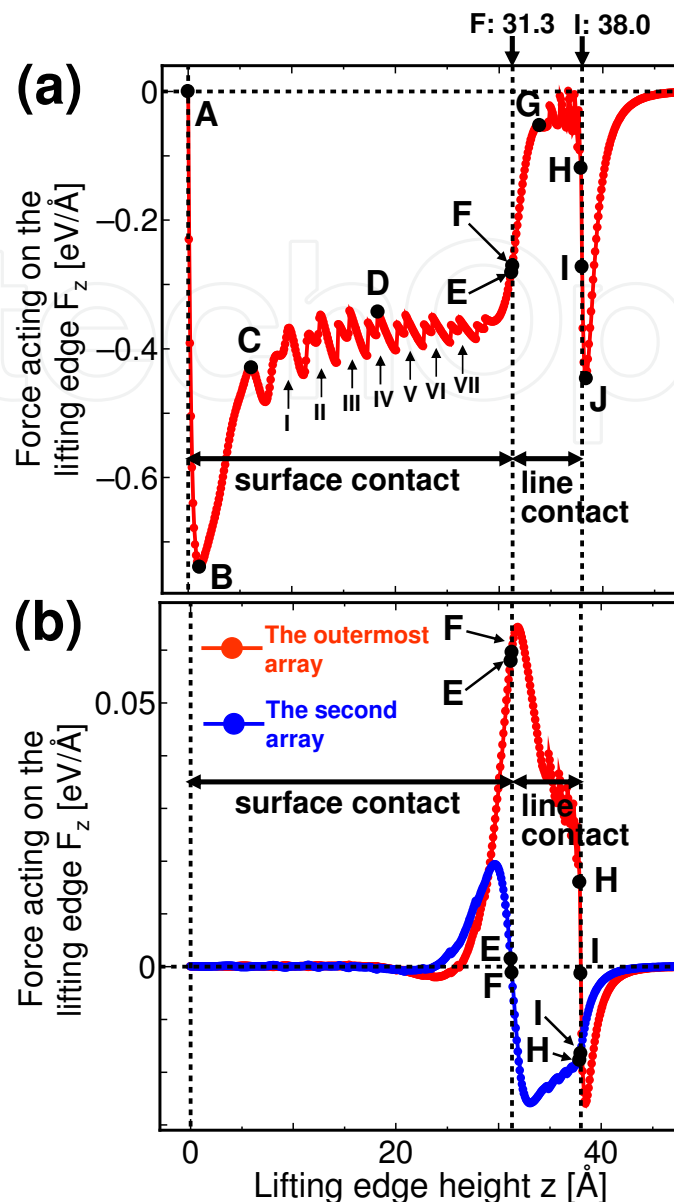
Fig. 9. (a) The vertical force F_z acting on the lifting edge, plotted as a function of the lifting edge height z for the graphene with armchair-type free edge. The indices A-J correspond to those of Fig. 8. (b) The red-colored averaged force per one atom acting on the outermost array, and the blue-colored one acting on the second array, as a function of the lifting edge height z [Å]. The indices E, F, H and I correspond to those of Figs. 8 and 9(a).

Line-contact region After the surface contact vanishes, the line contact appears [Fig. 8F]. Here the 'line contact' is defined by the following two criteria similar to the case of the center-lifting peeling: 1) The outermost array of the free edge of the graphene sheet [Fig. 1(b)] receives the averaged repulsive interaction force per one carbon atom from the graphite surface. 2) The second array next to the outermost array [Fig. 1(b)] receives the averaged attractive interaction force per one carbon atom. As illustrated in Fig. 9(b), the edge height z = 31.3 Å satisfies the above criteria [Fig. 8F]. Here the free edge adsorbed onto the graphite surface is nearly fixed even if the left edge is lifted [Fig. 8F → Fig. 8G: z = 33.9 Å]. As a result the in-plane bending of the graphene sheet markedly decreases, and $|F_z|$ decreases to zero

[Figs. 9(a)F-G]. After that the free edge slides on the surface until the graphene sheet takes planar structure within the y-z plane [Fig. 8H: z = 37.9 Å], where $|F_z|$ increases again [Fig. 9(a)H].

Toward complete peeling Then the graphene sheet is continuously moved upward [Fig. 8I: z = 38.0 Å $\rightarrow$ Fig. 8J: z = 38.4 Å], and is completely peeled from the surface. It is noted the line contact clearly vanishes at z = 38.0 Å [Fig. 9(b)I]. The attractive interaction force $|F_z|$ increases to take the maximum value [Figs. 9(a)I $\rightarrow$ J], and then it gradually decreases to zero toward the complete peeling.

4.2 Atomic-scale sliding within lateral plane

Fig. 9(a) shows the atomic-scale zigzag structures within the surface- and line-contact regions, which can be explained by the following atomic-scale sliding motions of the graphene sheet within the x-y plane.

Surface-contact region During the surface contact region between C and E in Fig. 9(a), z-F_z curve takes the atomic-scale zigzag structures from I to VII. The zigzag behaviors exhibit the transition from the continuous [Figs. 10(a)I - II] to the sawtooth shapes [Figs. 10(a)III - VII]. First Figs. 10(a)1 $\rightarrow$ 2 $\rightarrow$ 3 $\rightarrow$ 4 $\rightarrow$ 5 correspond to Figs. 10(b) 1 $\rightarrow$ 2 $\rightarrow$ 3 $\rightarrow$ 4 $\rightarrow$ 5, which show that the graphene sheet continuously slides passing over the nearest neighboring AB stacking sites with the graphite surface. The trajectories of the graphene sheet exhibit the continuous zigzag paths as shown in Fig. 10(b)5. Next Figs. 10(a) 6 $\rightarrow$ 7 $\rightarrow$ 8 $\rightarrow$ 9 $\rightarrow$ 10 correspond to Figs. 10(c) 6 $\rightarrow$ 7 $\rightarrow$ 8 $\rightarrow$ 9 $\rightarrow$ 10 which show that the graphene sheet takes the zigzag stick-slip motions between the nearest neighboring AB stacking sites. Just before the slip, the graphene sheet deviates quite a little from the AB-stacking site [Fig. 10(c)6: z = 17.3 Å]. Then it discretely jumps or slips to the neighboring AB-stacking site [Fig. 10(c)7: z = 17.4 Å]. As the peeling proceeds, the graphene sheet continuously slides quite a little [Fig. 10(c)8: z = 18.2 Å], then it discretely slips again to the neighboring AB stacking site [Fig. 10(c)9: z = 18.3 Å]. After that the graphene sheet continuously slides quite a little again [Fig. 10(c)10: z = 20.1 Å] until the next slip toward the neighboring AB stacking site occurs. As a result the trajectories of the graphene sheet exhibit the discrete zigzag paths connecting the nearest neighboring AB-stacking sites as shown in Fig. 10(c)10. The period of the zigzag behavior of the F_z curve decreases from 3.7Å to 2.5 Å as shown in Fig. 10(a) as the peeling proceeds. The lattice spacing of the graphite surface, 2.5 Å, appears in the peeling force curve particularly for the stick-slip region.

Line-contact region During the line contact region between G and H in Fig. 9(a), z-F_z curve takes another atomic-scale zigzag structures as shown in Fig. 11(a). One of the zigzag behaviors in the force curve [Figs. 11(a) 1 $\rightarrow$ 2 $\rightarrow$ 3] corresponds to the stick-slip sliding motions of the graphene sheet [Figs. 11(b) 1 $\rightarrow$ 2 $\rightarrow$ 3]. Here the free edge of the graphene sheet slides with nearly the straight stick-slip motions. One of the carbon atoms on the free edge passes over the carbon-carbon bonds as shown in Figs. 11(b)1 and 3.

5. Edge-lifting case of zigzag-edge graphene

Recently it has been reported that the edge structure of the graphene sheet plays quite an important role in electronic, magnetic and optical properties of graphene, which can be also expected to give influences on the mechanical properties such as the peeling process. Therefore, in this section, the peeling process of the graphene sheet with zigzag edge is
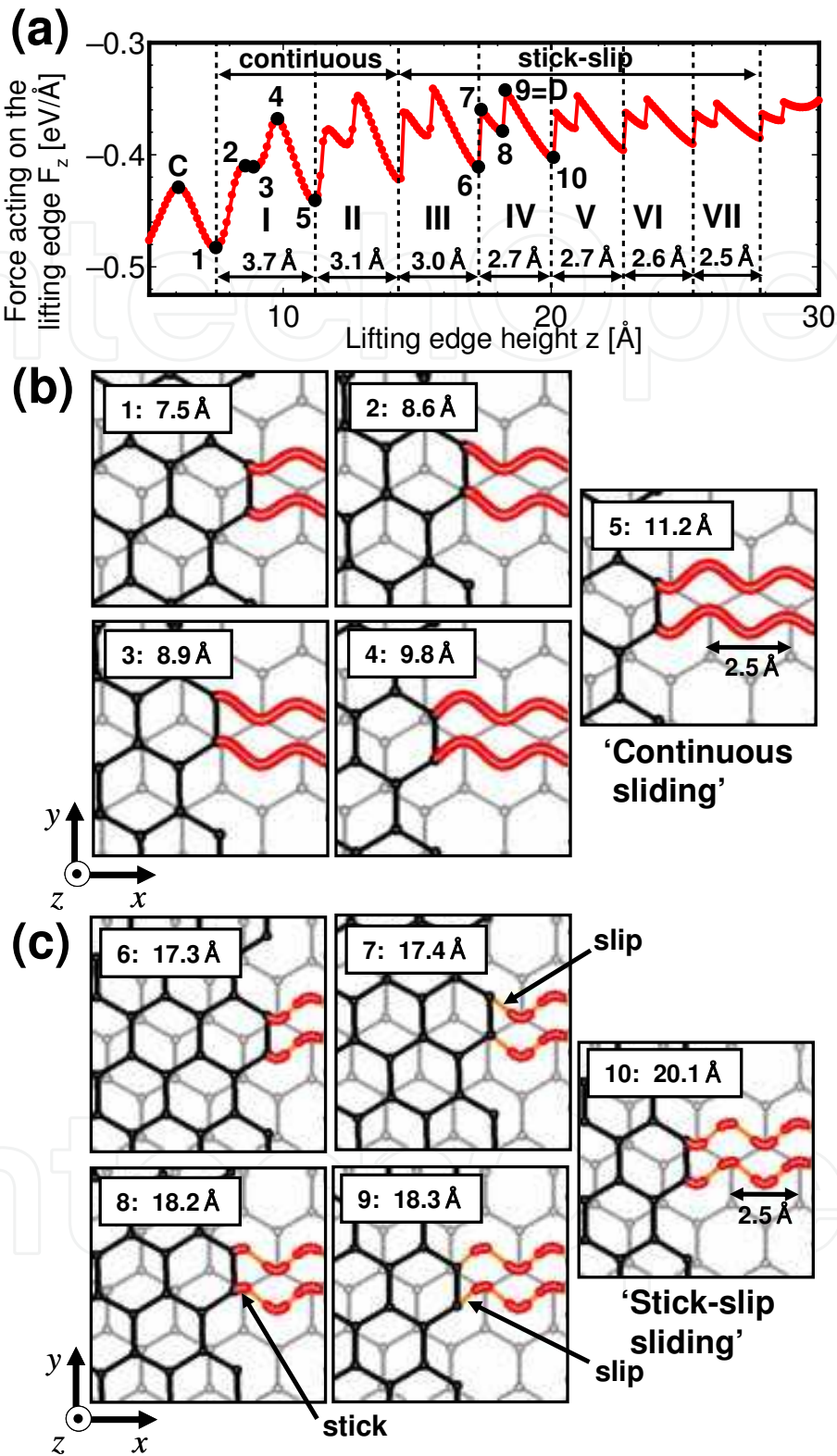
Fig. 10. (a) Enlargement of part of the z - F_z curve (Fig. 9(a)) corresponding to the continuous and stick-slip process during the surface contact. (b) The trajectories of the two carbon atoms on the free edge from 1 to 5 indicated in (a). (c) The trajectories of the two carbon atoms on the free edge from 6 to 10 indicated in (a).
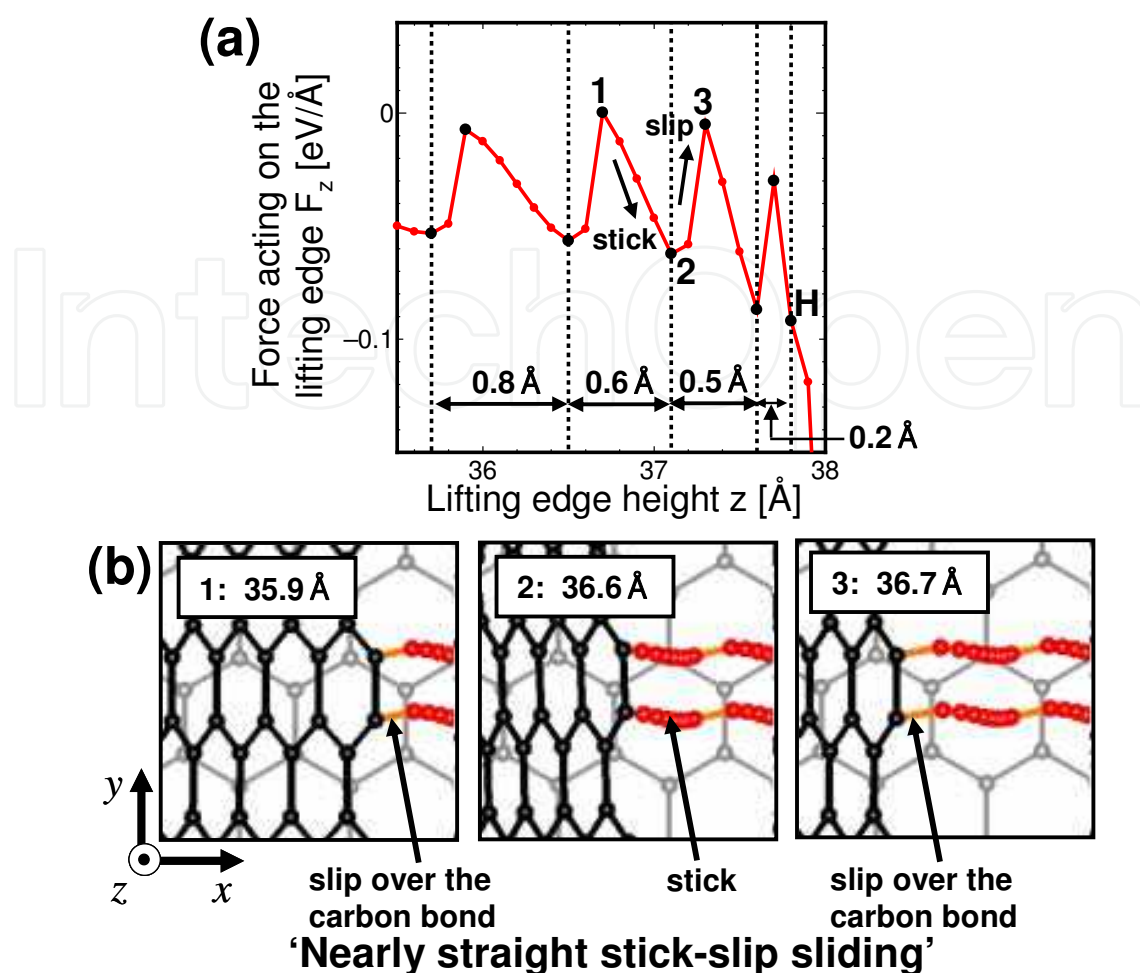
Fig. 11. (a) Enlargement of part of the z - F_z curve (Fig. 9(a)) corresponding to the nearly straight stick-slip region during the line contact. (b) The trajectories of the two carbon atoms on the free edge from 1 to 3 indicated in (a).

discussed. In the simulation, the model obtained by rotating Fig. 1(b) by 30° is used [Fig. 1(c)], and the left zigzag edge is lifted to simulate the peeling process, while the right free edge is zigzag type. As a result, the nanoscale peeling process within the x-z plane and the global shape of the force curve [Fig. 12] is similar to Figs. 8 and 9, respectively. The qualitative tendency of the decrease of the period and amplitude of the force curve [Fig. 12I-IV] is similar to that for Fig. 9(a)I-VII. However the details of the atomic-scale mechanics of the zigzag edge are clearly different from those of the armchair edge as follows:

During the surface contact, the graphene sheet first takes zigzag [Figs. 13(b)1-6] and then straight stick-slip motions [Figs. 13(c)7-11], passing over the nearest neighboring AB-stacking site along [10$\overline{1}$0] direction. It is noted, to avoid AA-stacking registry, the graphene sheet takes zigzag slip toward the nearest neighboring AB-stacking site as shown in Fig. 13(b)1 → 2, although it then takes straight slip as shown in Fig. 13(c)7 → 8. The minimum period of the force curve of 4.4 Å [Fig. 13(a)IV] reflects the lattice period of the graphite surface along the [10$\overline{1}$0] direction, while 2.5 Å for the armchair-type edge [Fig. 10(a)VII] reflects that along the [12$\overline{3}$0] direction. Thus the edge structure gives the marked effects on the atomic-scale dynamics depending on the lattice orientation of the surface.
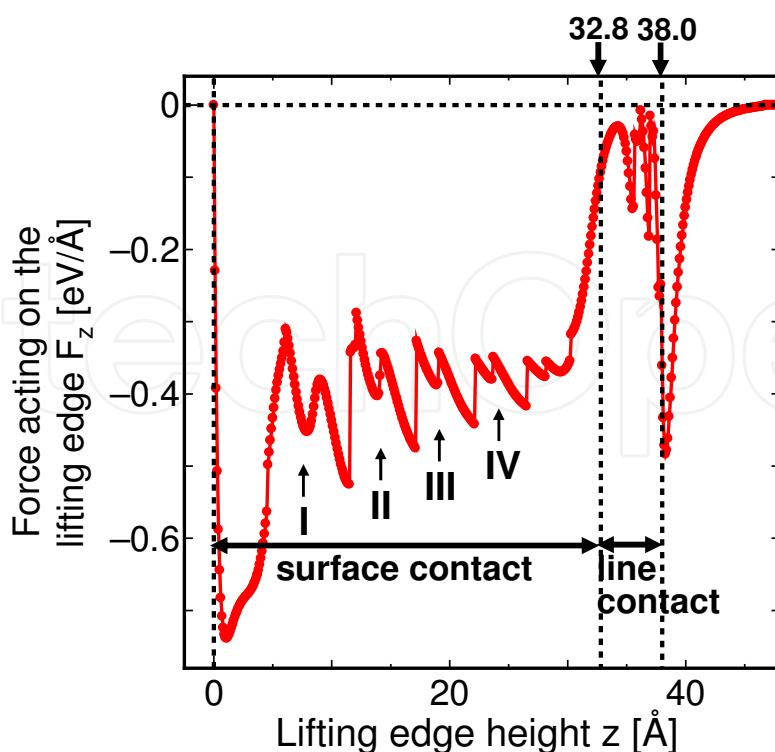
Fig. 12. The vertical force F_z acting on the lifting edge, plotted as a function of the lifting edge height z for the graphene with zigzag-type free edge

During the line contact, the difference between the armchair- and zigzag-type edge is enhanced. Fig. 14(a) reflects the zigzag stick-slip motion of the graphene sheet [Figs. 14(b)1-9] unlike nearly the straight stick-slip motion [Figs. 10(b)1-3]. Important point of the line-contact sliding is that each carbon atom on the free edge takes stick-slip motion between the nearest neighboring six-membered rings. When each atom is located on the hollow site of the six-membered ring, the graphene sheet does not deform along the y direction [Figs. 14(b)1, 4-5, and 8-9]. However, when each atom is located a little far from the hollow site or near the carbon bond, the graphene sheet bends toward the y direction to decrease the total interaction energy [Figs. 14(b)2-3 and 6-7]. Thus, in the case of the zigzag-type edge, collective motion of the single carbon 'atom' on the free edge nearly dominates the graphene mechanics together with its deformation. On the other hand, for the armchair-type edge, collective motion of the single carbon 'bond' is dominant.

6. Discussions and conclusions

In this chapter molecular mechanics study of the nanoscale peeling of the monolayer graphene sheet has been performed. The peeling force curve clearly exhibits the change of the graphene shape from the surface- to the line-contact.

In Section 3, the peeling of the monolayer graphene sheet with the armchair edge for lifting the center position is discussed. It is noted that the maximum lateral sliding force $F_x \approx 0.1$ eV/Å is only about 3 % of the absolute value of the maximum adhesion force $|F_z| \approx 3.1$ eV/Å. This small sliding force F_x is derived from the superlubricity at the interface between the graphene sheet and the graphite surface (Sasaki et al., 2007) and atomic-scale wear (Sasaki et al., 2009c). There is possibility that such anisotropy between the vertical
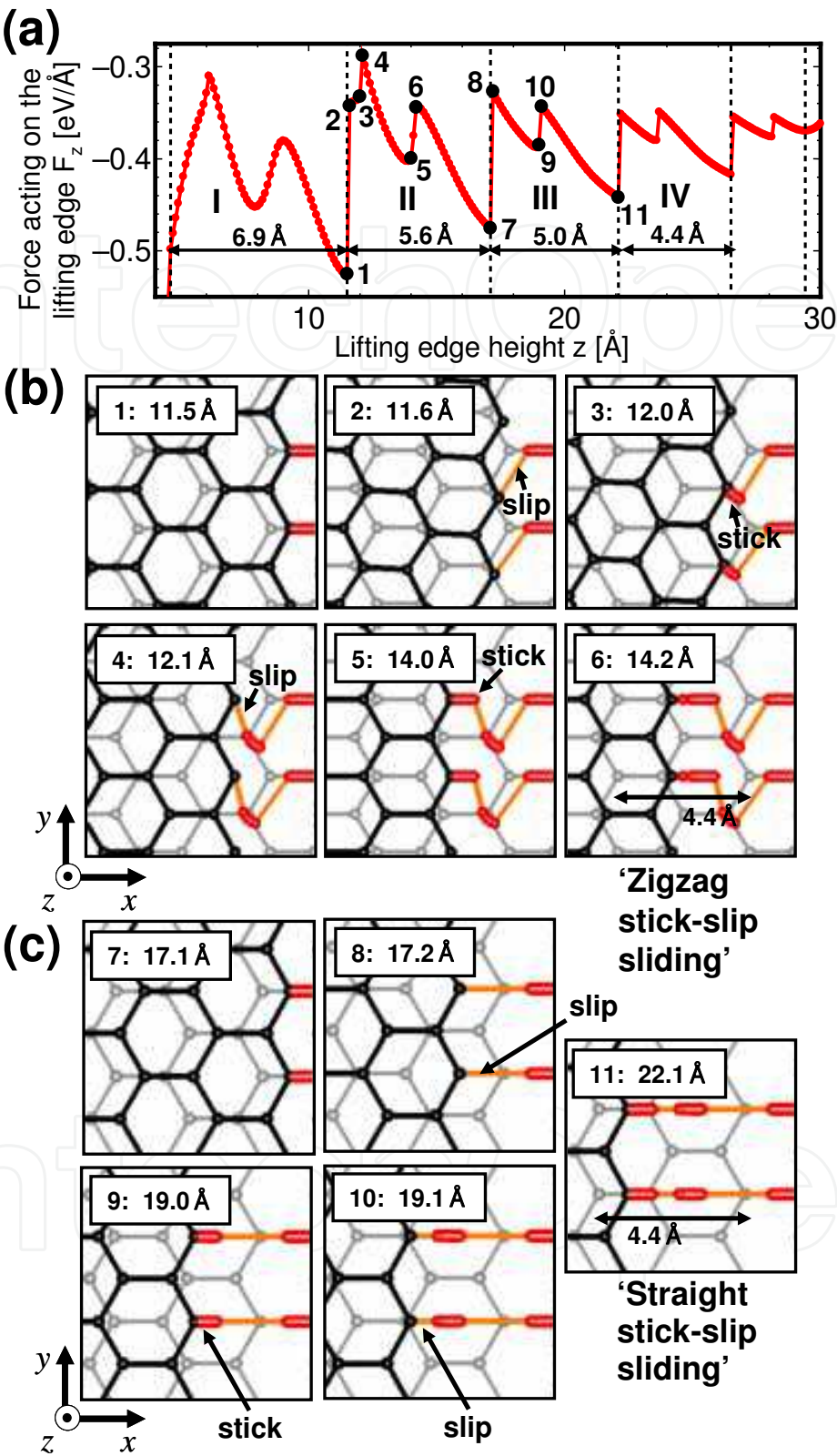
Fig. 13. (a) Enlargement of part of the *z* - *F_z* curve (Fig. 12(b)) corresponding to the zigzag and straight stick-slip process during the surface contact. (b) The trajectories of the two carbon atoms on the free edge from 1 to 6 indicated in (a). (c) The trajectories of the two carbon atoms on the free edge from 7 to 11 indicated in (a).
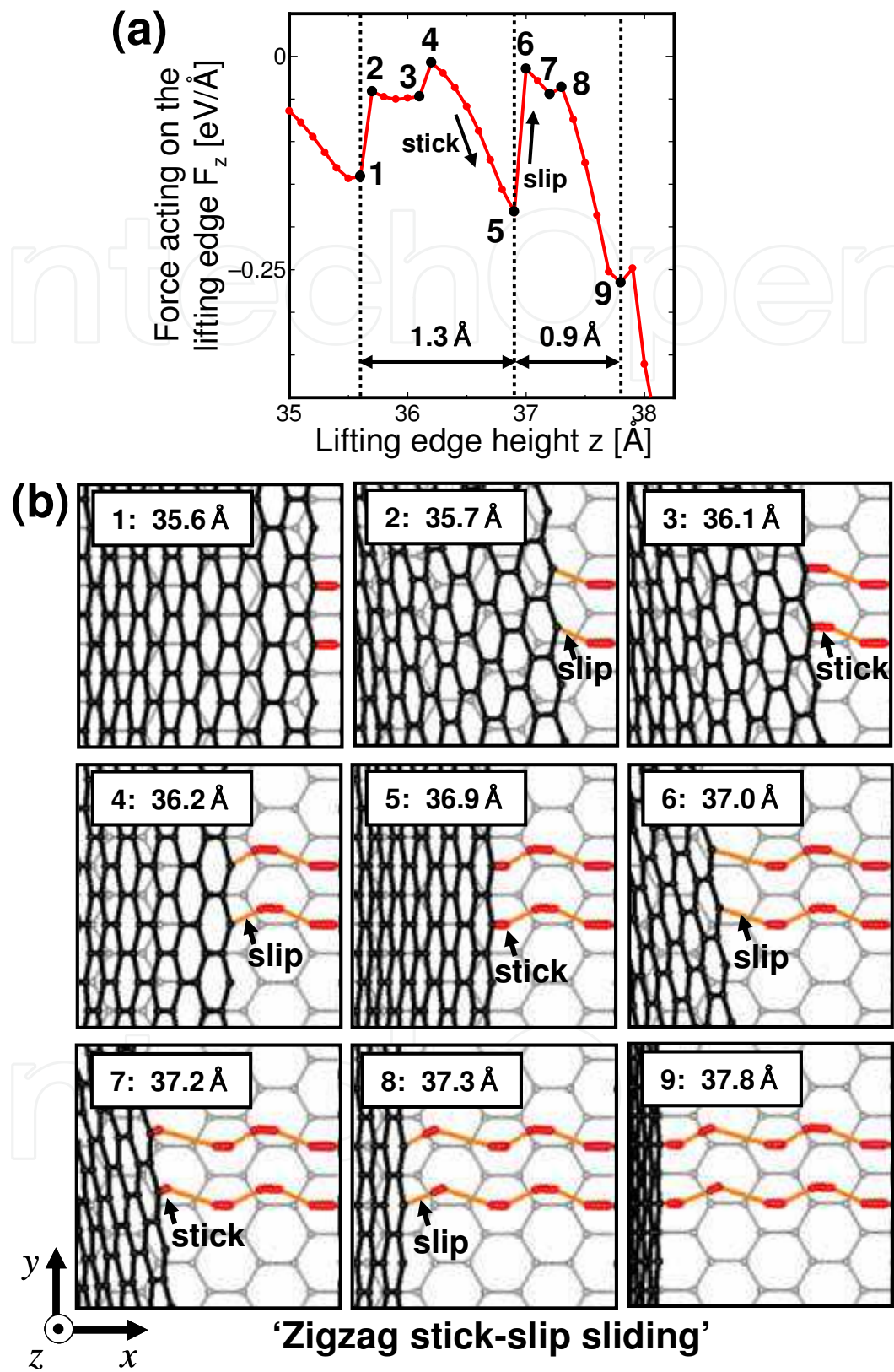
Fig. 14. (a) Enlargement of part of the z - F_z curve (Fig. 12(b)) corresponding to the zigzag stick-slip process during the line contact. (b) The trajectories of the two carbon atoms on the free edge from 1 to 9 indicated in (a).

force F_z and the lateral sliding force F_x can be applied to the adhesives, which can be strongly adhered to the substrate but can easily slide on it. Our AFM measurement exhibits that the maximum pull-off force is about several hundreds of nN, which is clearly much larger than the binding force, 3 eV/Å≈ 4.8 nN, assumed in our simulation.

In Secs. 4 and 5, the peeling of the monolayer graphene sheet with the armchair- and zigzag-edge for lifting the edge position is discussed, respectively. The atomic-scale sliding motion of the monolayer graphene sheet during the peeling process is found. For the graphene sheet with armchair edge, the transition from the continuous to the stick-slip motion of the graphene sheet is found, which can be explained as follows: The peeling process induces the increase of the peeled area of the graphene sheet, and the decrease of the surface contact area. Considering the peeled area of the graphene sheet acts as an effective spring as shown in Fig. 15, the increase of the peeled area makes the effective spring softer, and the decrease of the surface contact area decreases the energy barrier to slide the graphene sheet. Finally the peeling process induces the transition from the continuous to the stick-slip sliding motion of the graphene sheet, together with the decrease of the period and amplitude of the z-F_z curve. Important point is that the period of the peeling force curve for the armchair-edge graphene for the surface contact region corresponds to the lattice spacing of the graphite surface along $[12\overline{3}0]$ direction, 2.5 Å. On the other hand, for the zigzag-edge graphene, the period becomes the lattice spacing along $[10\overline{1}0]$ direction, 4.4 Å. This means the sliding length of the graphene sheet along x direction becomes nearly equal to the peeled length along z direction. The zigzag structures of the peeling force curve with the same period of about several Å have been also observed by our preliminary experiments using the multilayered graphene, which will be reported elsewhere. Of course, if the number of the peeled graphene sheets is reduced, the direct comparison between the present simulation and the experiment will become possible.

As a result, the center-lifting case requires the largest attractive peeling force, -3.1 eV/ Å, in order to peel the graphene sheet as shown in Fig. 16(a). On the other hand, the edge-lifting case requires only -0.74 eV/Å, about 20 % of that for the center-lifting case as shown in Figs. 16(b) and 16(c). The edge structures give little influences on the basic features of the force curve. However, the sliding direction and the edge structure clearly gives marked influences on the surface- and line-contact regions, respectively.

Another important point is that the behavior of the lateral force curve $F_x(z)$ is qualitatively the same as that of the vertical force curve $F_z(z)$ during the surface contact as shown in Fig. 9(b). Therefore it can be said that the peeling force curve, $F_z(z)$, directly reflects the atomic-scale friction force, $F_x(z)$, which decreases to 0.019 eV/Å≈ 30 pN for z = 27.8 Å [Fig. 9(b)]. This ultralow friction force F_x is derived from the superlubricity at the interface between the graphene sheet and the graphite surface (Sasaki et al., 2007, 2009c, Itamura 2009a, 2009b) . Furthermore effect of the edge structure on the peeling process is clarified by comparison of the free edge between the armchair- and zigzag-types. As mentioned above, the atomic-scale structure of the force curve during the surface contact reflects the lattice spacing of the graphite surface. So the minimum period of the atomic-scale structure of the force curve can tell us the atomic-scale lattice orientation and structure of the free edge of graphene. Such information can be used for the control of the electronic properties of the graphene sheet adsorbed onto the substrate. Therefore this paper indicates the possibility of the identification of the lattice orientation and the edge structure of the graphene sheet.
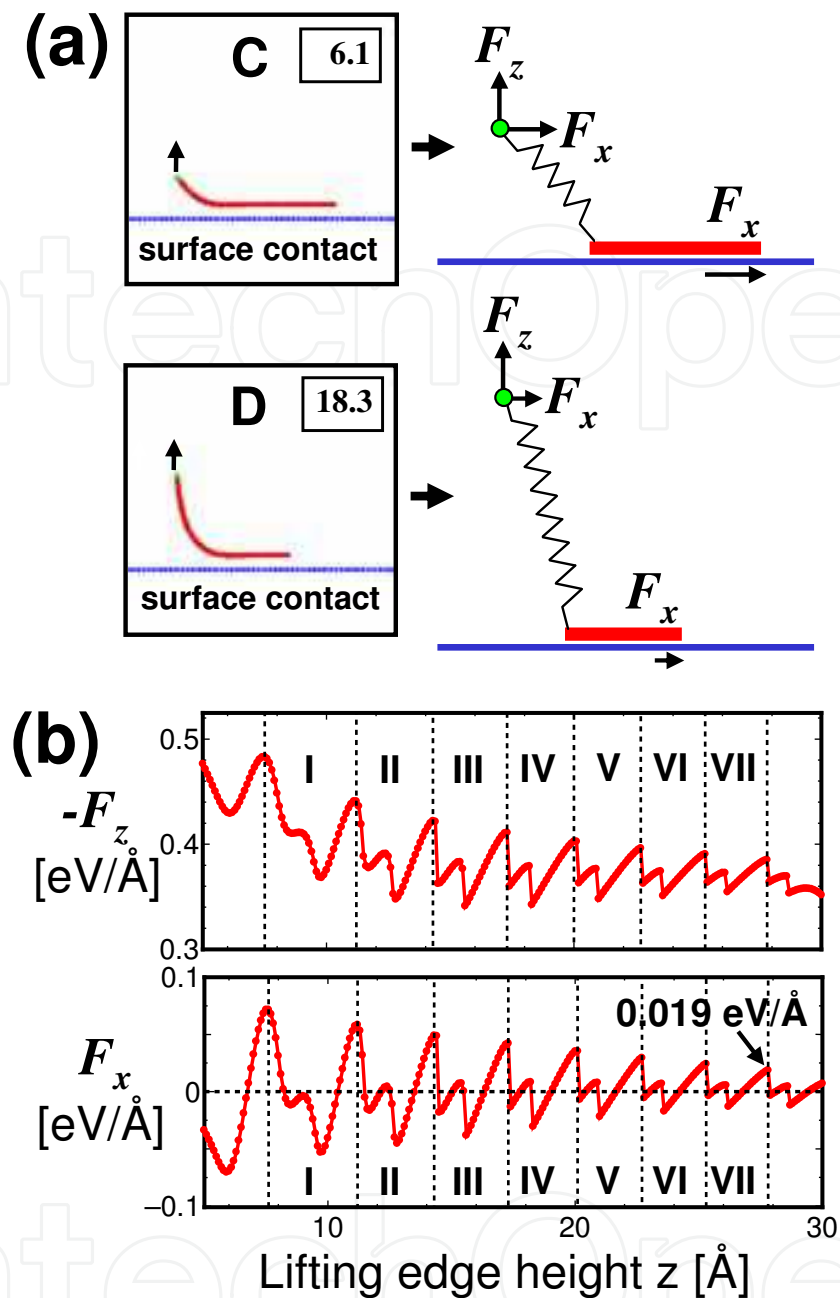
Fig. 15. (a) Schematic illustration of the increase of the peeled area and the decrease of the surface contact area from C (z = 6.1 Å) to D (z = 18.3 Å) for the graphene sheet with armchair-type free edge. (b) – F_z and F_x plotted as a function of the edge height z, show qualitatively the same behavior to each other for the graphene sheet with armchair-type free edge.

In this chapter, we discussed the importance of the dynamics of the free edge during the peeling process. On the other hand, we also found the importance of the shape of the graphene sheet. Additional simulated model and results are shown in Fig. 17. As shown in Fig. 17(a), rectangular graphene sheet whose aspect ratio is different from that of the graphene
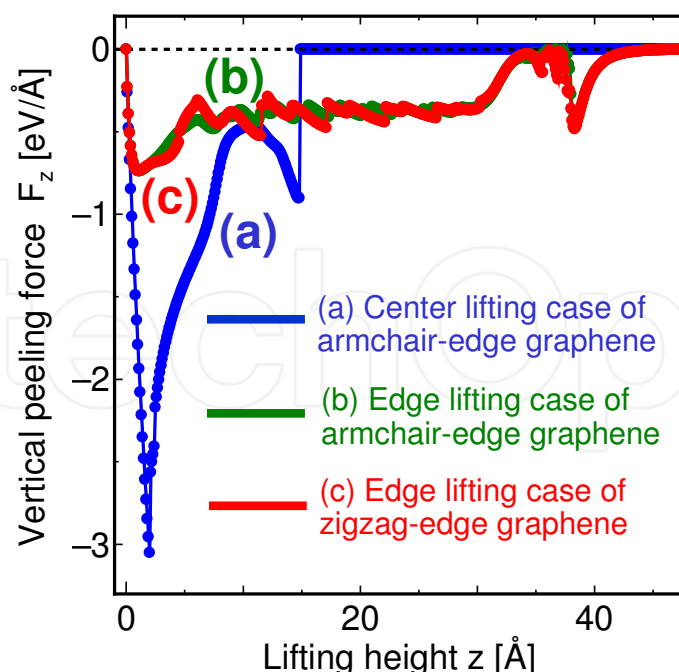
Fig. 16. Comparison of the vertical forces, F_z, among (a) center-lifting case of the armchair-edge graphene sheet, (b) edge-lifting case of the armchair-edge graphene sheet, and (c) edge-lifting case of the zigzag-edge graphene sheet.

sheet of Fig. 1(b) is used. The basic shape of the vertical force curve, Fig. 17(b), is similar to that of Fig. 3. However the armchair type edge is peeled first for Fig. 17(a), although the zigzag type edge is peeled first for Fig. 1(b) as discussed in Section 3. This means that the shape of the graphene sheet plays an important role for deciding which edge is peeled first. Effect of the graphene shape on the peeling process will be discussed in detail somewhere in the near future.

Lastly it should be noted that the peeling process discussed in this chapter is closely related to the atomic-scale wear of the graphite and the graphene tip formation in the friction force microscopy (Sasaki et al., 2009c). When the tip is pushed onto the surface for less than the critical tip height, the outermost graphene layer is attached to the FFM tip, which results in the formation of the graphene tip. In that case, the graphene sheet takes the surface contact with the second layer graphene, and it takes the two-dimensional stick-slip motion. However it is difficult to observe directly the stick-slip motion during the scan process, due to the very small gap between the FFM tip and the graphite surface. On the other hand, if the peeling process is used, it can be expected that the contact at the AFM tip/graphite interface has a wider space to be observed directly by ex. Transmission Electron Microscopy (TEM). This paper indicates the possibility of a direct observation of the stick-slip motion of the graphene sheet, that's to say, the elementary process of the atomic-scale friction or superlubricity which occurs at the tip/graphite surface interface.
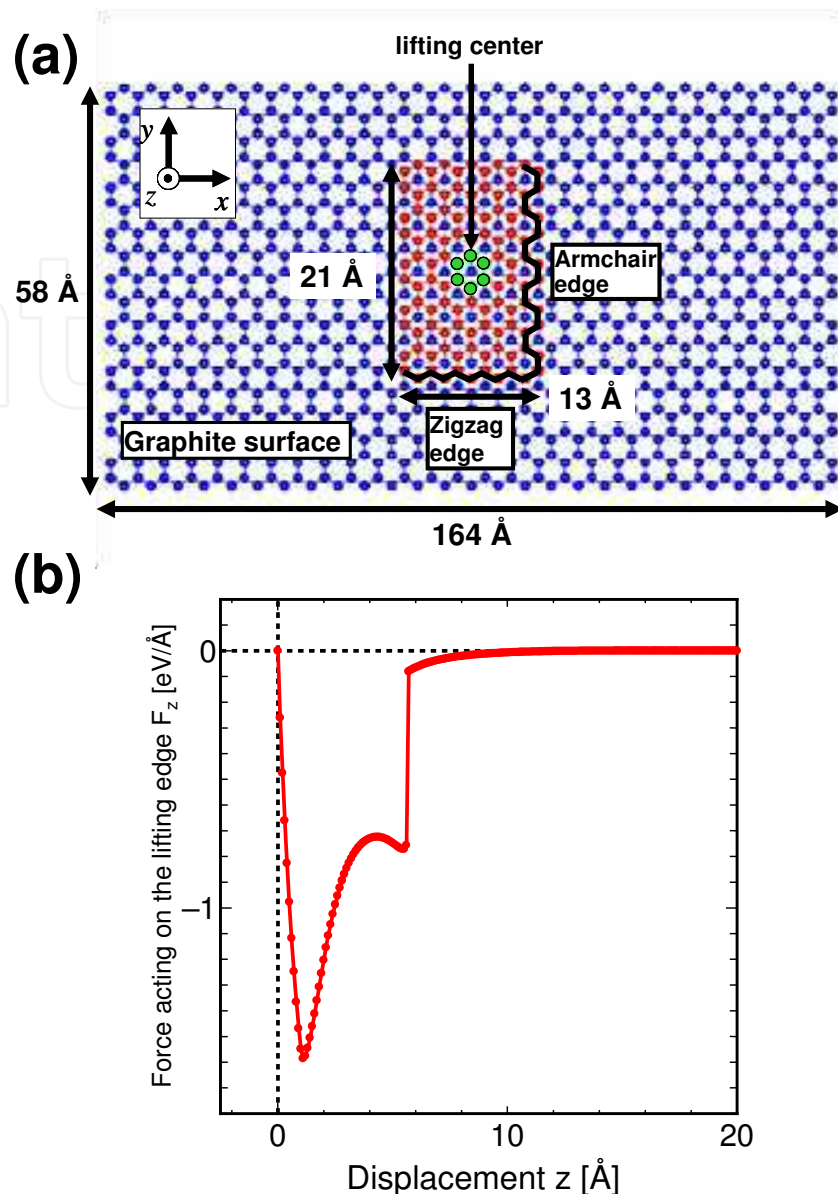
Fig. 17. (a) The model of the red-colored monolayer graphene sheet physically adsorbed onto the blue-colored rigid graphite surface within the x – y plane. The green-colored six-membered ring at the center position is moved upward along the z (or [0001]) direction, by z = 0.1 Å. Initial AB stacking registry of the red-colored graphene sheet with the blue-colored graphite surface is assumed. (b) The vertical force F_z acting on the center six-membered ring, plotted as a function of the lifting displacement z.

## 7. References

Autumn, K., Liang, Y. A., Hsieh, S. T., Zesch, W., Chan, W. P., Kenny, T. W., Fearing, R., & Full, R. J. (2000). Adhesive force of a single gecko foot-seta. *Nature*, Vol. 405, No. 6 (June, 2000) 681-685, ISSN 0028-0836 (print), 1476-4687 (online)

Autumn, K., Sitti, M., Liang, Y. A., Peattie, A. M., Hansen, W. R., Sponberg, S., Kenny, T. W., Fearing, R., Israelachvili, J. N. & Full, R. J. (2002). Evidence for van der Waals

adhesion in gecko setae. *Proc. Natl. Acad. Sci. U.S.A.*, Vol. 99, No. 19 (September, 2002) 12252-12256

Geim, A. K. and Novoselov, K. S. (2007). The rise of graphene. *Nature Mat.*, Vol. 6, No. 3 (March, 2007) 183-191, ISSN 1476-1122 (print), 1476-4660 (online)

Ishikawa, M., Kato, M., Harada, R., Sasaki, N. & Miura, K. (2008). Visualization of nanoscale peeling of carbon nanotube on graphite. *Appl. Phys. Lett.*, Vol. 93, No. 8 (August, 2008) 0831221-0831223, ISSN 0003-6951 (print), 1077-3118 (online)

Ishikawa, M., Harada, R., Sasaki, N. & Miura, K. (2009). Adhesion and peeling forces of carbon nanotubes on a substrate. *Phys. Rev. B.*, Vol. 80, No. 19 (November, 2009) 1934061-1934064, ISSN 1098-0121 (print), 1550-235x (online)

Itamura, N., Miura, K., & Sasaki, N., (2009a). Analysis of Mechanism of Low Lateral Stiffness of Superlubic C_{60} Bearing System. *Jpn. J. of Appl. Phys.*, Vol. 48, (March, 2009) 0302141-0302143, ISSN 0021-4922 (print), 1347-4065 (online)

Itamura, N., Miura, K., & Sasaki, N., (2009b). Simulation of Scan-Directional Dependence of Superlubricity of C_{60} Molecular Bearings and Graphite. *Jpn. J. of Appl. Phys.*, Vol. 48, (June, 2009) 0602071-0602073, ISSN 0021-4922 (print), 1347-4065 (online)

Lu, J. P., Li, X. -P. & Martin, R. M. (1988). Ground state and phase transitions in solid C_{60}. *Phys. Rev. Lett.*, Vol. 68, No. 10 (March, 1992) 1551-1554, ISSN 0031-9007 (print), 1079-7114 (online)

Novoselov, K. S., Geim, A. K., Morozov, S. V., Jiang, D., Zhang, Y., Dubonos, S. V., Grigorieva, I. V. & Firsov, A. A. (2004). Electric Field Effect in Atomically Thin Carbon Films. *Science,* Vol. 306, No. 5696 (October, 2004) 666-669, ISSN 0036-8075 (print), 1095-9203 (online)

Novoselov, K. S., Geim, A. K., Morozov, S. V., Jiang, D., Katsnelson, M. I., Grigorieva, I. V., Dubonos, S. V. & Firsov A. A. (2005). Two-dimensional gas of massless Dirac fermions in graphene. *Nature,* Vol. 438, No. 11 (November, 2005) 197-200, ISSN 0028-0836 (print), 1476-4687 (online)

Press, W. H., Teukolsky, S. A., Vetterling, W. T. & Flannery, B. P. (1999). Sec. 10.6 Minimization or Maximization of Functions, In: *Numerical Recipes in FORTRAN : The Art of Scientific Computing, 2nd ed.*, 413-418, Cambridge Univ. Press, ISBN 0-521-43064-X, New York

Qu, L., Dai, L., Stone, M., Xia, Z. & Wang, Z. L. (2008). Carbon Nanotube Arrays with Strong Shear Binding-On and Easy Normal Lifting-Off. *Science,* Vol. 322, No. 5899 (October, 2008) 238-242, ISSN 0036-8075 (print), 1095-9203 (online)

Sasaki, N., Toyoda, A., Saitoh, H., Itamura, N., Ohyama, M. & Miura, K., (2006). Theoretical Simulation of Atomic-Scale Peeling of Single-Walled Carbon Nanotube from Graphite Surface. *e-J. Surf. Sci. Nanotech.*, Vol. 4, (January, 2006) 133-137, ISSN 1348-0391

Sasaki, N., Itamura, N. & Miura, K. (2007). Simulation of Atomic-Scale Ultralow Friction of Graphite/C_{60}/Graphite Interface along [1010] Direction. *Jpn. J. of Appl. Phys.*, Vol. 46, No. , (December, 2007) L1237-L1239, ISSN 0021-4922 (print), 1347-4065 (online)

Sasaki, N., Toyoda, A., Itamura, N. & Miura, K., (2008). Simulation of Nanoscale Peeling and Adhesion of Single-Walled Carbon Nanotube on Graphite Surface. *e-J. Surf. Sci. Nanotech.*, Vol. 6, (February, 2008) 72-78, ISSN 1348-0391

Sasaki, N., Okamoto, H., Itamura, N. & Miura, K., (2009a). Peeling of Graphene Sheet -
        Simulation Study. *e-J. Surf. Sci. Nanotech.*, Vol. 7, (July, 2009) 783-786, ISSN 1348-
        0391

Sasaki, N., Saitoh, H., Itamura, N. & Miura, K., (2009b). Analysis of Lateral Orientation of
        Single-Walled Carbon Nanotube on Graphite. *e-J. Surf. Sci. Nanotech.*, Vol. 7,
        (January, 2009) 48-52, ISSN 1348-0391

Sasaki, N., Saitoh, H., Terada, K., Itamura, N. & Miura, K., (2009c). Simulation of Atomic-
        Scale Wear of Graphite - Nanotip Induced Graphene Formation. *e-J. Surf. Sci.
        Nanotech.*, Vol. 7, (March, 2009) 173-180, ISSN 1348-0391

Sasaki, N., Okamoto, H., Itamura, N. & Miura, K., (2010). Atomic-Scale Friction of
        Monolayer Graphenes with Armchair- and Zigzag-Type Edges During Peeling
        Process. *e-J. Surf. Sci. Nanotech.*, Vol. 8, (March, 2010) 105-111, ISSN 1348-0391

Stoddard, S. D. and Ford, J. (1973). Numerical Experiments on the Stochastic Behavior of a
        Lennard-Jones Gas System. *Phys. Rev. A,* Vol. 8, No. 3 (September, 1973) 1504-1512,
        ISSN 1050-2947 (print), 1094-1622 (online)

Tersoff, J., (1988). Empirical Interatomic Potential for Carbon, with Applications to
        Amorphous Carbon. *Phys. Rev. Lett.,* Vol. 61, No. 25 (December, 1988) 2879-2882,
        ISSN 0031-9007 (print), 1079-7114 (online)
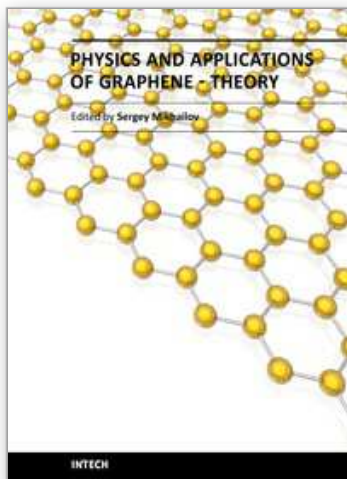
Physics and Applications of Graphene - Theory

Edited by Dr. Sergey Mikhailov

The Stone Age, the Bronze Age, the Iron Age... Every global epoch in the history of the mankind is characterized by materials used in it. In 2004 a new era in material science was opened: the era of graphene or, more generally, of two-dimensional materials. Graphene is the strongest and the most stretchable known material, it has the record thermal conductivity and the very high mobility of charge carriers. It demonstrates many interesting fundamental physical effects and promises a lot of applications, among which are conductive ink, terahertz transistors, ultrafast photodetectors and bendable touch screens. In 2010 Andre Geim and Konstantin Novoselov were awarded the Nobel Prize in Physics "for groundbreaking experiments regarding the two-dimensional material graphene". The two volumes Physics and Applications of Graphene - Experiments and Physics and Applications of Graphene - Theory contain a collection of research articles reporting on different aspects of experimental and theoretical studies of this new material.

How to reference

In order to correctly reference this scholarly work, feel free to copy and paste the following:

Naruo Sasaki, Hideaki Okamoto, Shingen Masuda, Kouji Miura and Noriaki Itamura (2011). Simulated Nanoscale Peeling Process of Monolayer Graphene Sheet - Effect of Edge Structure and Lifting Position, Physics and Applications of Graphene - Theory, Dr. Sergey Mikhailov (Ed.), ISBN: 978-953-307-152-7, InTech, Available from: http://www.intechopen.com/books/physics-and-applications-of-graphene-theory/simulated-nanoscale-peeling-process-of-monolayer-graphene-sheet-effect-of-edge-structure-and-lifting

INTECH

open science | open minds